JOURNAL OF VIROLOGY, June 2009, p. 5796–5805 Vol. 83, No. 11
0022-538X/09/$08.00+0 doi:10.1128/JVI.02471-08

Suppression of *Bamboo Mosaic Virus* Accumulation by a Putative Methyltransferase in *Nicotiana benthamiana*▽

Chun-Wei Cheng, Yi-Yuong Hsiao,† Hui-Chuan Wu, Chi-Mau Chuang, Jao-Shien Chen, Ching-Hsiu Tsai, Yau-Heiu Hsu, Yao-Chu Wu, Cheng-Cheng Lee, and Menghsiao Meng*

Graduate Institute of Biotechnology, National Chung Hsing University, 250 Kuo-Kuang Rd., Taichung, Taiwan 40227, Republic of China

Received 2 December 2008/Accepted 10 March 2009

Bamboo mosaic virus **(BaMV) is a 6.4-kb positive-sense RNA virus belonging to the genus *Potexvirus* of the family *Flexiviridae*. The 155-kDa viral replicase, the product of ORF1, comprises an N-terminal *S*-adenosyl-L-methionine (AdoMet)-dependent guanylyltransferase, a nucleoside triphosphatase/RNA 5′-triphosphatase, and a C-terminal RNA-dependent RNA polymerase (RdRp). To search for cellular factors potentially involved in the regulation of replication and/or transcription of BaMV, the viral RdRp domain was targeted as bait to screen against a leaf cDNA library of *Nicotiana benthamiana* using a yeast two-hybrid system. A putative methyltransferase (PNbMTS1) of 617 amino acid residues without an established physiological function was identified. Cotransfection of *N. benthamiana* protoplasts with a BaMV infectious clone and the PNbMTS1-expressing plasmid showed a PNbMTS1 dosage-dependent inhibitory effect on the accumulation of BaMV coat protein. Deletion of the N-terminal 36 amino acids, deletion of a predicted signal peptide or transmembrane segment, or mutations in the putative AdoMet-binding motifs of PNbMTS1 abolished the inhibitory effect. In contrast, suppression of PNbMTS1 by virus-induced gene silencing in *N. benthamiana* increased accumulation of the viral coat protein as well as the viral genomic RNA. Collectively, PNbMTS1 may function as an innate defense protein against the accumulation of BaMV through an uncharacterized mechanism.**

Bamboo mosaic virus (BaMV) is a flexuous-rod positive-sense RNA virus belonging to the genus *Potexvirus* of the family *Flexiviridae*. The 6.4-kb genome contains five open reading frames (ORFs), with a 5′ methyl cap and a 3′ poly(A) tail (27). Two major subgenomic RNAs of 2 and 1 kb are produced upon viral infection in host cells. The protein product of ORF1, translated from the genomic RNA, is a 155-kDa viral replicase comprising an N-terminal capping enzyme domain (23), a helicase-like domain harboring nucleoside triphosphatase/RNA 5′-triphosphatase activities (24), and a C-terminal RNA-dependent RNA polymerase (RdRp) (22). The capping enzyme domain exhibits an *S*-adenosyl-L-methionine (AdoMet)-dependent guanylyltransferase activity, which is characteristic of the capping enzyme in members of alphavirus superfamily (2, 3, 17, 28). Following the 5′-γ-phosphate-removed activity of the viral nucleoside triphosphatase/RNA 5′-triphosphatase, the capping enzyme domain is responsible for cap structure formation at the 5′-diphosphate end of the viral RNAs (11), while the viral RdRp domain plays a central role in viral replication and transcription.

Viruses encode limited number of proteins, and hence they need to recruit host proteins to aid in the various steps of the viral infection, including entry, gene expression, replication, virion assembly, and release. Elucidating the interactions between viruses and their hosts is thus a necessary task toward understanding the complete life cycle of the viruses. In regard to the replication of positive-strand RNA viruses, cellular factors of the host RNA-processing and translational machinery are often recruited for use in the viral replication complex (1, 20). For example, translation elongation factors Ts, Tu, and ribosomal protein S1 are components of the replicase complex of RNA bacteriophage Qβ (5), while EF-1α (functionally homologous to bacterial Tu), EF-1β, and EF-1γ (homologous to bacterial Ts) bind tightly to the viral RNA polymerase of *Vesicular stomatitis virus* (8). Poly(A)-binding protein, the other component of host translational machinery, was also found in association with RdRp of *Zucchini yellow mosaic potyvirus* (32). Moreover, eIF1A was found to bind the RNAs of *Tobacco mosaic virus* (TMV) (34, 37), *Turnip yellow mosaic virus* (12), *West Nile virus* (4), and *Dengue virus* (9). Recently, genome-wide screens have identified a wide variety of cellular factors capable of affecting the replication of *Brome mosaic virus* and *Tomato bushy stunt virus* in yeast (18, 29). These factors are diverse, and many of them are involved in the metabolism of proteins, nucleic acids, and lipids. With respect to BaMV, binding of the chloroplast phosphoglycerate kinase to the 3′ untranslated region was found to be required for efficient accumulation of BaMV coat protein in *Nicotiana benthamiana* (26).

A yeast two-hybrid screen was used to identify cellular factors from a leaf cDNA library of *N. benthamiana* by using the RdRp domain of BaMV as bait in this study. A putative methyltransferase was discovered, and its involvement in the accumulation of BaMV was investigated.

MATERIALS AND METHODS

cDNA library construction. Total RNA was isolated by first pouring 80°C extraction buffer, consisting of equal volumes of phenol (pH 4.3) and 0.1 M Tris

* Corresponding author. Mailing address: Graduate Institute of Biotechnology, National Chung Hsing University, 250 Kuo-Kuang Rd., Taichung, Taiwan 40227. Phone: 886-4-22840328, ext. 636. Fax: 886-4-22853527. E-mail: mhmeng@dragon.nchu.edu.tw.

† Present address: National Museum of Marine Biology and Aquarium, 2 Houwan Road, Checheng, Pingtung, 94450, Taiwan.

▽ Published ahead of print on 18 March 2009.

(pH 8.0) buffer that also contained 0.1 M LiCl, 10 mM EDTA, and 1% sodium dodecyl sulfate (SDS), into liquid nitrogen-frozen and powdered leaves of *N. benthamiana* in the ratio of 1 g leaf to 5 ml extraction buffer. After vigorous shaking for 30 s, 1/5 volume of chloroform was included, and the mixture was shaken again for another 30 s. The RNA in the aqueous phase was precipitated with ethanol after repeated extraction with chloroform. The mRNA therein was then isolated using PolyATract mRNA isolation systems (Promega). Procedures for cDNA synthesis, including first-strand synthesis by Moloney murine leukemia virus reverse transcriptase (RT), second-strand synthesis by DNA polymerase I, ligation to EcoRI adaptor, and cDNA fractionation by gel filtration (collecting those with sizes of 0.5 to 2 kb), were according to the manual provided by Stratagene. After treatment with XhoI, the pool of cDNA fragments was inserted into pYESTrp2 (Invitrogen) downstream from the coding regions of the V5 epitope, nuclear localization signal (NLS), and B42 activation domain and transformed into *Escherichia coli* T10F′. The cDNA library was completed after collecting pYESTrp2 cDNAs from approximately 3.5×10^4 *E. coli* transformants.

Yeast two-hybrid screening. The Hybrid-hunter system, in which an interaction between bait and prey proteins would activate the expression of *his3* and *lacZ* genes in *Saccharomyces cerevisiae* strain L40, was used in this study. Competent cell preparation, transformation, and selection of yeast colonies were guided by the user manual provided by Invitrogen. First, the cDNA region for RdRp domain (amino acids 908 to 1365 of BaMV replicase) was amplified from a BaMV infectious clone by PCR using specified primers with added SacI and SalI sites at their 5′ termini, respectively. After treatment with the restriction endonucleases, the amplified 1.4-kb DNA fragment was inserted in frame into SacI-SalI-cleaved pHybLex/Zeo for the production of the bait on which LexA was fused to the N terminus of the RdRp domain. The L40 expressing the bait was then transformed with the pool of pYESTrp2-cDNAs and spread on YC-WHUK/Z300 selection agar plates. Colonies grown on the selection plates were further analyzed for β-galactosidase activity based on both filter and quantitative assays. Plasmid DNAs were then isolated from those with significant β-galactosidase activity and transformed into *E. coli* T10F′. Each pYESTrp2-cDNA propagated in *E. coli* was isolated and retransformed into bait-expressing yeast cells to confirm the potential protein interaction. The nucleotide sequences of the selected cDNA fragments were finally determined with the ABI Prism 3100 autosequencer (Perkin-Elmer).

Protein expression vectors in protoplasts. The authentic 5′ fragment of PNbMTS1 was obtained by 5′ rapid amplification of cDNA ends (RACE) using two internal reverse primers, 5′-AGGAACATTAGCATAGTAC and 5′-GGA ACGTCATAGCTCGATC, with the SMART RACE kit (Clontech). The full-length cDNA of PNbMTS1 was then substituted for β-glucuronidase cDNA in the transient-expression vector pBI221 (Clontech) to become pBI-PNbMTS1 by using BamHI and SacI restriction sites. Mutation at Gly215/Gly217 and Gly302/Gly303, N-terminal deletion, and C-terminal addition with a sequence encoding a hemagglutinin (HA) tag (YPYDVPDYA) on pBI-PNbMTS1 were performed using specified pairs of divergent primers according to the protocol of the QuikChange site-directed mutagenesis kit (Stratagene). pBI-PNbMTS1/GFP, an expression vector for green fluorescent protein (GFP)-fused PNbMTS1, was created by changing the stop codon of PNbMTS1 on pBI-PNbMTS1 to an XhoI site and then inserting a GFP-coding region right after the cDNA of PNbMTS1 by using XhoI and SacI sites. For the transient expression of the BaMV RdRp domain in protoplasts, the cDNA of RdRp (1,419 nucleotides) was first substituted for the β-glucuronidase cDNA in pBI221 by using SmaI and SacI sites, and then a coding sequence for an HA tag was inserted at the 3′ end of RdRp cDNA by PCR according to QuikChange site-directed mutagenesis protocol (Stratagene).

Protoplast transfection. Preparation of *N. benthamiana* protoplasts and plasmid transfection were performed basically according to the protocol described by J. Sheen (31). In brief, protoplasts were prepared from approximately 25-day-old leaves. Transfection was conducted by adding the indicated amounts of plasmid DNA or viral RNA to 1×10^5 protoplasts in a total of 150 μl MMG buffer (0.55 M mannitol-MES [morpholineethanesulfonic acid][pH 5.7] and 15 mM $MgCl_2$). After addition of 150 μl 40% polyethylene glycol 4000, the mixture was incubated at room temperature for 30 min. The transfected protoplasts were then repeatedly washed with MMC (0.55 M mannitol-MES [pH 5.7] and 20 mM $CaCl_2$) and finally cultivated at room temperature in growth buffer (0.55 M mannitol-MES [pH 5.7], 1 μM $CuSO_4$, 1 μM KI, 1 mM $MgSO_4$, 0.2 mM K_2HPO_4, 1 mM KNO_3, 10 mM $CaCl_2$, and 30 μg/ml cefatoxime) for the indicated periods of time under a constant light.

VIGS. Virus-induced gene silencing (VIGS) was carried out as described by Ratcliff et al. (30), with plasmids pTRV1 and pTRV2 provided generously by D. C. Baulcombe. Briefly, a 5′-distal region of the PNbMTS1 ORF (480 bp) was amplified by PCR and cloned into pTRV2 to become pTRV2-PNbMTS1. *Agrobacterium tumefaciens* C58C1, carrying either pTRV1 or pTRV2-PNbMTS1, was suspended in induction medium (130 μM acetosyringone, 10 mM $MgCl_2$) to an optical density at 600 nm of ~1.0 and incubated at room temperature for 3 h. These two types of cells were then mixed at a ratio of 1:1 and infiltrated into the undersides of the first two true leaves of *N. benthamiana* at the four-leaf stage using a 1-ml needleless syringe. Control plants received the same treatment except that pTRV2-PNbMTS1 was replaced by pTRV2. An inoculation of 0.5 μg BaMV virion was given to the sixth true leaf when it was fully developed. Finally, the virus-infected leaf was harvested for BaMV coat protein and RNA transcript analysis at the third day postinoculation.

Protein analysis. Protein concentrations in cell extracts were determined with the bicinchoninic acid reagent (Pierce) by using bovine serum albumin as the standard. The relative amounts of the large subunit of ribulose-1,5-bisphosphate carboxylase (L-RuBisCo) in protein samples were estimated by the intensity of the Coomassie blue-stained protein bands on a 12% SDS-polyacrylamide gel electrophoresis (PAGE) using Multigauge imaging analysis software (Fujifilm). The viral coat proteins and HA-tagged proteins were detected by Western blot analysis using specific coat protein antisera raised in rabbit and commercial anti-HA antibodies (Sigma), respectively. The resulting data were processed using Image Station 2000 MM (Kodak).

Coimmunoprecipitation. Yeast cells harboring the indicated plasmids were suspended in yeast lysis buffer (50 mM Tris [pH 8.0], 150 mM NaCl, 1% NP-40, 1 mM phenylmethylsulfonyl fluoride) and disrupted at 4°C by vigorous mixing with acid-treated glass beads (0.3 to 0.45 mm). The supernatant of the extracts was precipitated with mouse anti-V5 or rabbit anti-LexA antibodies (Invitrogen) and protein A-Sepharose. The pellets were then dissolved in protein loading buffer and subjected to Western blot analysis using anti-LexA or anti-V5 antibodies, respectively, as the primary antibodies. As for protoplasts, the cells were harvested at 18 h posttransfection and disrupted at 4°C in 50 mM Tris (pH 8.0), 15 mM $MgCl_2$, 120 mM KCl, 0.1% (vol/vol) β-mercaptoethanol, 20% (vol/vol) glycerol, 1 μM pepstatin, and 1 mM phenylmethylsulfonyl fluoride. Cell disruption was carried out with an ultrasonic disruptor with pulse intermittently on and off at 10-s intervals for 15 min. The debris was removed by centrifugation at $5{,}000 \times g$ for 10 min, and the membrane fraction (P30) was subsequently precipitated at $30{,}000 \times g$. P30 was then suspended in yeast lysis buffer, and the proteins in the supernatant were collected after another 1 h of centrifugation at $30{,}000 \times g$. Rabbit anti-GFP antibody and protein A-Sepharose were added into the supernatant, and the precipitated proteins were analyzed by Western blotting using mouse anti-HA antibody as the primary antibody.

β-Galactosidase activity assay. For filter assay, yeast cells grown on agar medium were transferred to filter paper and then disrupted by repeated freezing and thawing. The paper was then soaked in 100 mM phosphate (pH 7.0), 10 mM KCl, 1 mM $MgSO_4$, and 1 mg/ml X-Gal (5-bromo-4-chloro-3-indolyl-β-D-galactopyranoside) until color developed. For quantitative assay, 100 μl of disrupted cells was added to 900 μl reaction buffer as described above except that X-Gal was replaced with 0.64 mg/ml *o*-nitrophenyl β-galactoside. After incubation at 30°C for ~10 h, the optical density at 420 nm was determined with a spectrophotometer.

RdRp activity assay. P30 prepared from transfected protoplasts according to the protocol described above was subjected to a gradient centrifugation with 20 to 60% sucrose in 50 mM Tris (pH 8) that also contained 10 mM NaCl, 1 mM EDTA, 5 mM β-mercaptoethanol, and 5% glycerol at $189{,}000 \times g$ for 4 h. Fractions 5 to 7 of a total of 10 from top to bottom were then collected. The endogenous RdRp activity was analyzed by adding ATP, GTP, and CTP (each at 5 mM); UTP (5 μM); 10 μCi [α-^{32}P]UTP, and 0.3% Sarkosyl to the collected samples, and the reaction was allowed to take place at 25°C for 1 h (6). The RNA products were separated by electrophoresis on a 1% agarose gel and detected by autoradiography.

mRNA analysis. Total RNA from 100 mg of leaf tissue or 10^6 protoplasts was first extracted using a TriSolusion Reagent Plus kit (GeneMark) and then treated with DNase I. The mRNA therein was then primed with 1 μg oligo(dT) for the first-strand cDNA synthesis using Moloney murine leukemia virus RT in a total of 25 μl. The cDNA preparation was next used as the template in RT-PCR or real-time PCR analyses. For each real-time PCR, 1 μl of 100-fold-diluted cDNA was used with Sybr Advantage qPCR Premix (Clontech) and the following paired primers: 5′-TGTGCTGAACGGGTTATGAG and 5′-ACTGCCAATTGTCCC CTACA for a 5′-distal fragment of BaMV genomic RNA (nucleotides 51 to 282), 5′-CATAACCCCCTACCCTGACGTCC and 5′-TAGTTTCCCATCTCAGGC CTGCAG for a 574-bp fragment located on the 3′ end of PNbMTS1, 5′-GCA GTACTGGAGCTGCCAAGGC and 5′-GTAACCCCATTCATTGTCGTACC for a 291-bp fragment of glyceraldehyde-3-phosphate dehydrogenase (GAPDH), and 5′-ACTGACTTTCATACAGGTGC and 5′-TACCTTCTTACTGACA

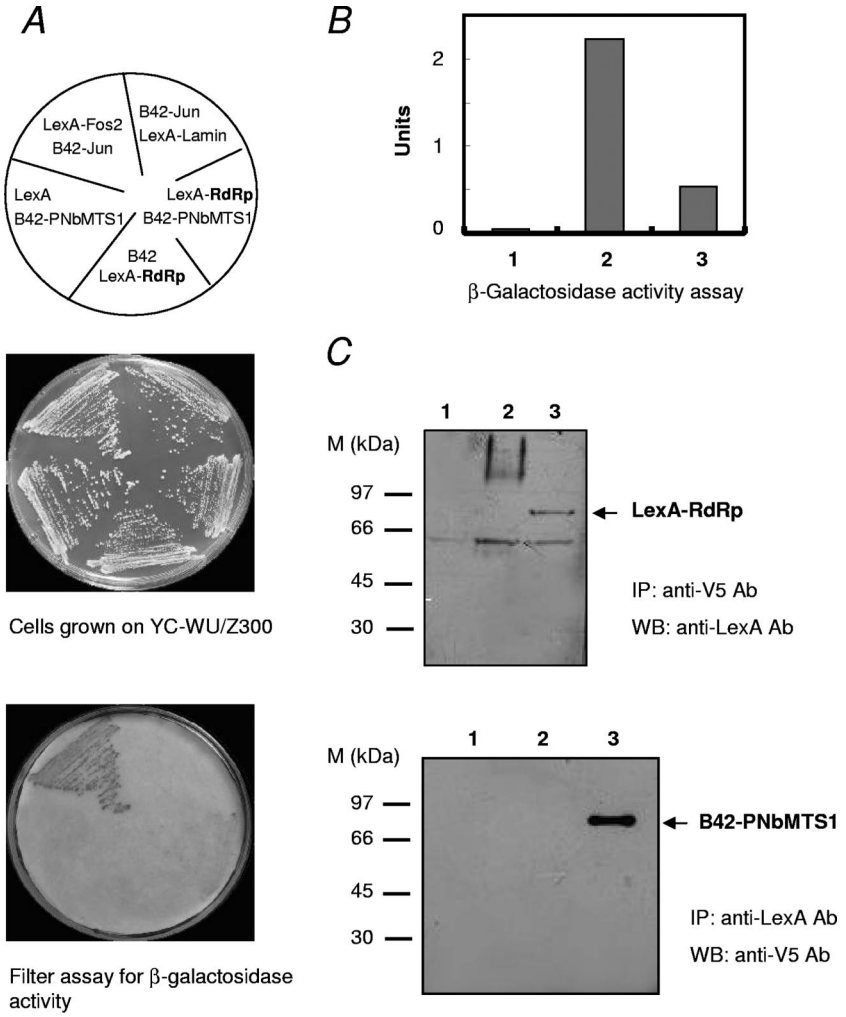

FIG. 1. Interaction between the BaMV RdRp domain and PNbMTS1 in yeast. (A) Yeast cells harboring various plasmid combinations as indicated were grown on YC-WU/Z300 medium and transferred to filter paper for β-galactosidase activity assay. Cells expressing LexA-Fos2 and B42-Jun were used as a positive control, while those expressing LexA-lamin and B42-Jun, LexA and B42-PNbMTS1, and B42 and LexA-RdRp were used as negative controls. The V5 epitope and NLS sequence fused in frame to the B42 activation domain were omitted for clarity. (B) Quantitative assay for β-galactosidase activity toward *o*-nitrophenyl β-galactoside was carried out as described in Materials and Methods. The overexpressed proteins in yeast cells in lanes 1, 2, and 3, are LexA-lamin and B42-Jun (negative control), LexA-Fos2 and B42-Jun (positive control), and LexA-RdRp and B42-PNbMTS1, respectively. (C) Extracts of yeast cells were first immunoprecipitated (IP) with antibodies (Ab) against V5 or LexA, and the precipitated proteins were subsequently analyzed by Western blotting (WB) using antibodies against LexA or V5, as indicated. Lanes 1, 2, and 3 represent extracts from cells expressing LexA-lamin and B42-Jun, LexA-Fos2 and B42-Jun, and LexA-RdRp and B42-PNbMTS1, respectively.

GCAC for a 213-bp fragment of the mitochondrial 18S RNA. PCR conditions were as follows: 1 cycle of 94°C for 5 min; 35 cycles of 94°C for 30 s, 58°C for 30 s, and 72°C for 30 s; and 1 cycle of 72°C for 1 min (except for PNbMTS1, for which the annealing temperature was set at 63°C). The signals generated by Sybr green with the reaction cycles were detected by Rotor-Gene 3000 (Corbett).

Nucleotide sequence accession number. The nucleotide sequence of PNbMTS1 has been submitted to GenBank under accession number EU563474.

RESULTS

Identification of PNbMTS1. To explore and understand the biological processes involved in modulating the replication of BaMV, the viral RdRp domain was chosen as a target for our study since it is this domain that actually performs the RNA replication process. The BaMV RdRp domain was fused to the LexA DNA-binding domain and used as bait to search for potential host factors using yeast two-hybrid screening against a leaf cDNA library of *N. benthamiana*. Interactions between the RdRp domain and potential host factors would activate His3 and LacZ expression. Of approximately 600 colonies originally identified on selection plates, 25 clones were found to possess the reproduced histidine auxotrophic phenotype and β-galactosidase activity. Nucleotide sequencing suggested that two of the cDNA clones were inserted downstream in frame with the coding regions of the V5 epitope, NLS, and B42 activation domain. One contains a putative methyltransferase, which we name pPNbMTS11, and was chosen for further investigation in this study. The activation of LacZ in yeast cells expressing LexA-RdRp and B42-PNbMTS1 was evident in both the filter and quantitative assays for β-galactosidase activity (Fig. 1A and B, respectively). To confirm the interaction between the bait and PNbMTS1, protein extracts of the re-

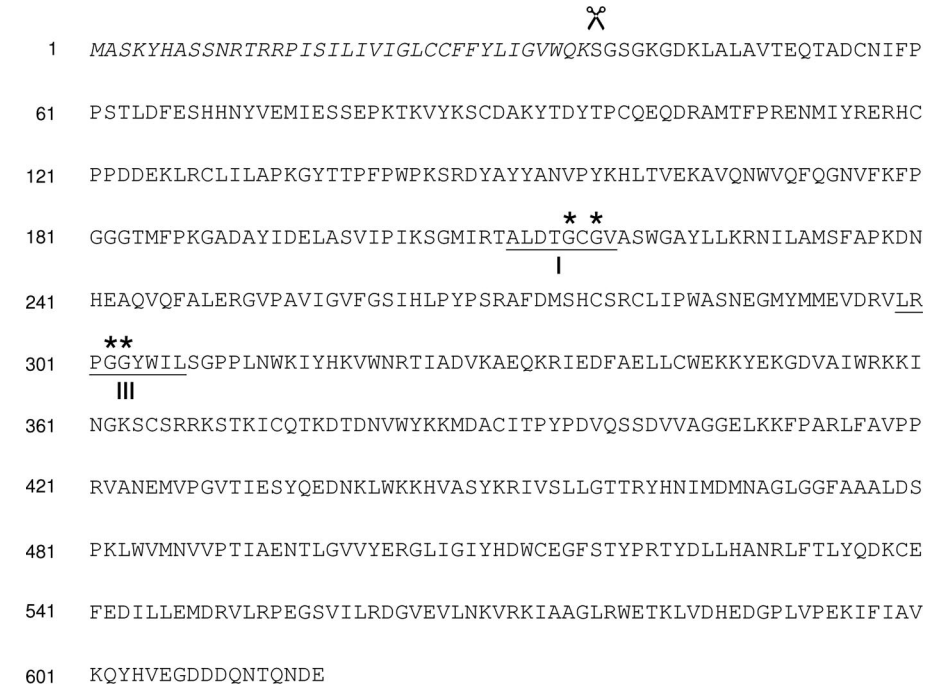

FIG. 2. Deduced amino acid sequence of PNbMTS1. The sequence in italic is predicted to be a transmembrane segment or signal peptide which may direct the protein to the mitochondrion or chloroplast. The underlined sequences are putative motifs I and III for AdoMet binding. The glycine residues denoted by asterisk were replaced with alanine in the mutant PNbMTS1 in this study. The scissors symbol indicates the cleavage site for the production of the N-terminally truncated protein.

combinant yeast cells were precipitated using anti-V5 or LexA antibodies and subsequently subjected to Western blot analysis using anti-LexA or V5 antibodies (Fig. 1C). The coimmunoprecipitation of the two proteins with both antibodies confirmed that the BaMV RdRp can interact with PNbMTS1.

5′ RACE was subsequently performed to complete the cDNA cloning of PNbMTS1 using two antisense primers as described in Materials and Methods. The full-length cDNA sequence of PNbMTS1 indicates that PNbMTS1 contains 617 amino acid residues (Fig. 2). The first 36 amino acid residues represent a transmembrane segment or a signal peptide that may direct the protein to the mitochondrion or chloroplast as predicted by web-based tools such as targetP (http://www.cbs.dtu.dk/services/TargetP/) and BaCelLo (http://gpcr.biocomp.unibo.it/bacello). BLAST analysis suggested that PNbMTS1 could be classified in a putative methyltransferase family, pfam03141, along with several similar proteins from plants such as *Arabidopsis*, rice, grape, potato, etc. (http://www.ncbi.nlm.nih.gov/blast/Blast.cgi). The biological functions of the proteins in this class are unknown, although dehydration responsiveness has been attributed to At4g18030, a family member from *Arabidopsis thaliana*, based on its similarity in amino acid sequence (~37% identity) to ERD3, an early-responsive-to-dehydration stress protein (16). Sequences similar to the consensus AdoMet-binding motifs I and III of a class of methyltransferases (13, 14) can be identified on PNbMTS1 at residues 211 to 218 and 299 to 307, respectively.

Function of PNbMTS1 in BaMV accumulation. To understand the role of PNbMTS1 in BaMV accumulation, the PNbMTS1 cDNA was substituted for the coding region of β-glucuronidase in plasmid pBI221, so that PNbMTS1 could be produced constitutively in *N. benthamiana* protoplasts. After cotransfection with pBI-PNbMTS1 and pCBG, which is a BaMV infectious clone containing an engineered cDNA copy of BaMV located downstream from the *Cauliflower mosaic virus* 35S promoter (10), the accumulation of BaMV coat protein in protoplasts was assayed at various time points. Introducing pBI-PNbMTS1 into protoplasts did not cause an apparent change in the total protein contents of the transfected protoplasts (Fig. 3A); however, an increase in the mRNA level of PNbMTS1 was evidenced by RT-PCR (Fig. 3B). Concomitantly, the accumulation of the viral coat protein decreased in response to the introduction of pBI-PNbMTS1 (Fig. 3C), suggesting that PNbMTS1 could interfere with the accumulation of BaMV. To know whether the viral replication machinery itself was affected by the overexpression of PNbMTS1, the viral RdRp activity in P30 fraction of protoplasts was measured using endogenous RNA templates. The results showed that the P30 from protoplasts cotransfected with pBI-PNbMTS1 produced smaller amounts of genomic as well as subgenomic RNA transcripts than that with the empty vector pBI221 (Fig. 3D), indicating that overexpression of PNbMTS1 indeed negatively affected the overall viral RdRp activity. Previous characterization of BaMV RdRp activity in P30 suggested that only viral RNAs in the replication complex could be used as templates for the endogenous RdRp activity assay (6). Therefore, the fact that fewer RNA transcripts were produced in the RdRp assay probably reflects a decrease of the viral replication complex. Nonetheless, the relative amounts of BaMV RdRp in different protoplast samples could not be determined at this time, because the viral replicase was too scarce to be detected by Western blot analysis (data not shown).

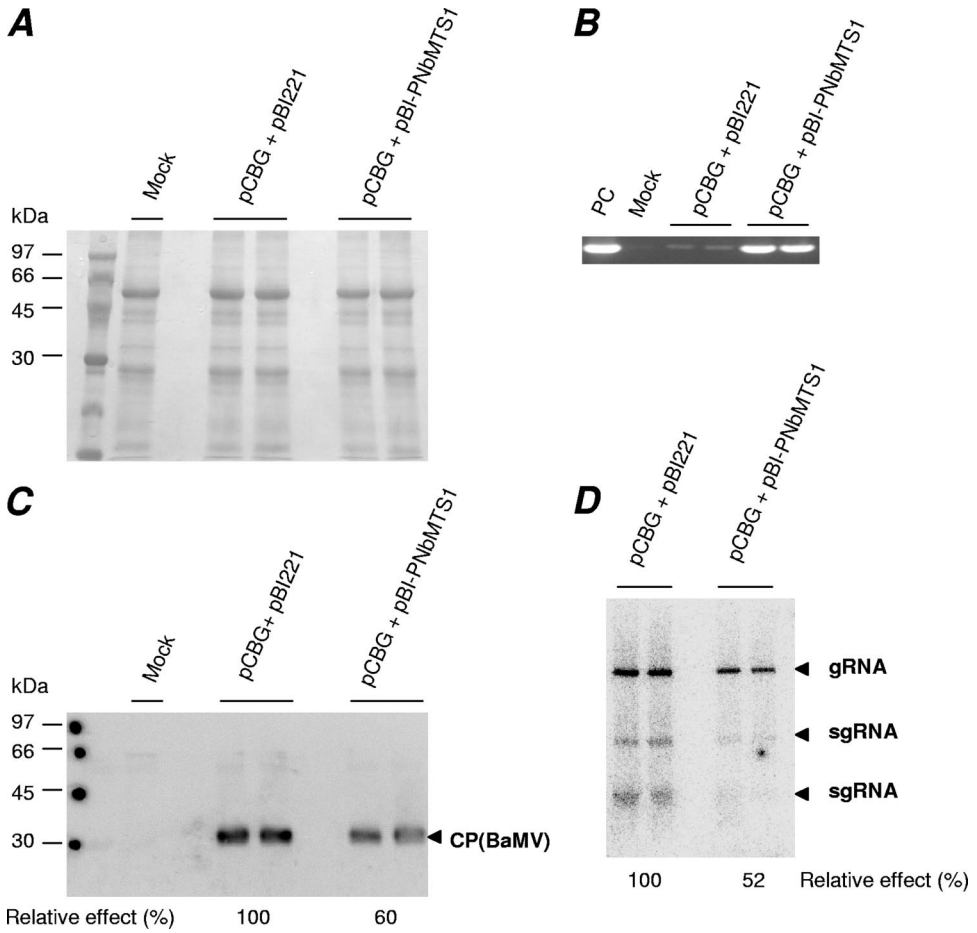

FIG. 3. Inhibition of BaMV accumulation by PNbMTS1. Protoplasts of *N. benthamiana* were transfected with 4 μg pCBG and 12 μg pBI221 or pBI-PNbMTS1 and incubated for 24 h at ambient temperature under a constant light as described in Materials and Methods. (A) Protein contents of protoplast extracts were analyzed by SDS-PAGE. (B) the PNbMTS1 transcript was analyzed by RT-PCR. PC, positive control using pBI-PNbMTS1 as the template in PCR. (C) BaMV coat protein (CP) accumulated in protoplasts was analyzed by Western blotting. (D) RdRp activity of the membrane fraction of protoplasts was assayed as described in Materials and Methods. gRNA and sgRNA, genomic and subgenomic RNAs, respectively. The relative effect was estimated based on the corresponding pixels of coat protein or genomic RNA. All the samples were from duplicate experiments (except mock).

To determine whether the inhibitory effect exerted by PNbMTS1 is concentration dependent, pCBG and increasing amounts of pBI-PNbMTS1 or pBI221 were introduced into protoplasts, and accumulation of BaMV coat protein was detected 16 h posttransfection. The results showed decreases in the accumulation of BaMV coat protein in the cotransfection combinations whenever pBI-PNbMTS1 was included (Fig. 4A). The results also suggested that the companion plasmids (pBI221 and pBI-PNbMTS1) could function as carriers to enhance the transfection efficiency of pCBG. To balance the carrier effect, pCBG was introduced along with a constant amount of companion plasmids, in which increasing amounts of pBI-PNbMTS1 were normalized with pBI221, into protoplasts. Indeed, accumulation of the coat protein at 16 h posttransfection decreased in a pBI-PNbMTS1 concentration-dependent fashion (Fig. 4B). Accumulation of BaMV coat protein in protoplasts was also measured as a function of incubation time. The inhibitory effect of PNbMTS1 on BaMV accumulation was apparent within the first 24 h but decreased by 48 h (Fig. 5). The decline of the inhibitory effect with incubation time might be attributed to BaMV genome replication and, as a result, BaMV would outnumber pBI-PNbMTS1 eventually during the incubation, rendering the influence of PNbMTS1 insufficient.

To quantify the effect of PNbMTS1 on BaMV accumulation, the amounts of the viral coat proteins in transfected protoplasts were analyzed by Western blotting (Fig. 6A) and calculated according to a standard curve of coat protein concentration versus pixels (Fig. 6B and C). It should be noted that the pixel values of the assayed samples are within the linear range of the standard curve. The coat protein accumulated up to 24.9 ± 3.5 ng per 10^5 cells after 16 h of cotransfection with 2.5 μg pCBG and 10 μg pBI221, whereas the amount reached only 9.9 ± 1.6 ng per 10^5 cells when pBI221 was replaced by pBI-PNbMTS1, indicating a ~60% reduction in the coat protein accumulation caused by PNbMTS1 under this culture condition (Fig. 6D).

Interaction of BaMV RdRp domain and PNbMTS1 in protoplasts. It was important to know whether the interaction between the BaMV RdRp domain and PNbMTS1 actually occurs in protoplasts. To overcome the difficulty of detecting the viral replicase in plant cells, the RdRp domain was tagged with an HA

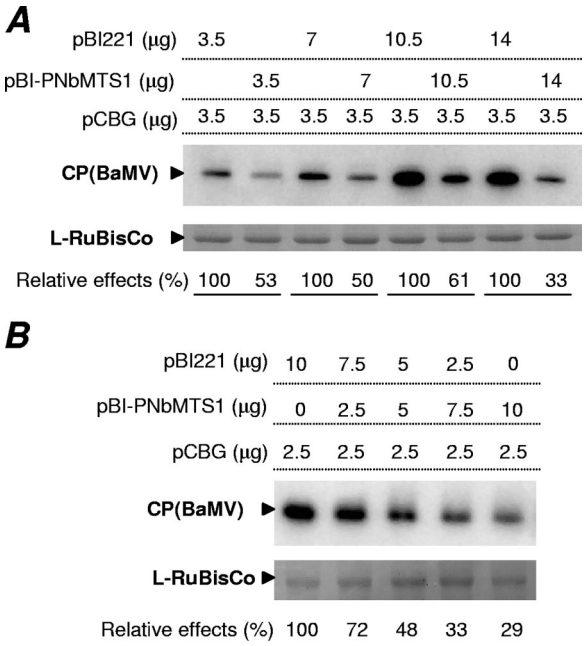

FIG. 4. Dosage dependence of the inhibitory effect of PNbMTS1 on BaMV accumulation. Protoplasts of *N. benthamiana* were transfected with pCBG and pBI221 or pBI-PNbMTS1 as indicated. After 16 h of incubation, the cell extracts were subjected to SDS-PAGE and Western blot analyses for total protein contents and accumulation of BaMV coat protein [CP(BaMV)], respectively. The relative effects were estimated based on the corresponding pixels of coat proteins after normalization to the amounts of ribulose-1,5-bisphosphate carboxylase (L-RuBisCo). The comparisions of coat protein accumulation were between cells transfected with the same amounts of pBI-PNbMTS1 and pB1221 (A) but among cells transfected with increasing amounts of pBI-PNbMTS1 (B).

epitope and expressed in protoplasts. After coexpression with PNbMTS1/GFP fusion protein, the cell extracts were precipitated with rabbit anti-GFP antibody, and the pellet was then analyzed by Western blotting using mouse anti-HA antibody as the primary

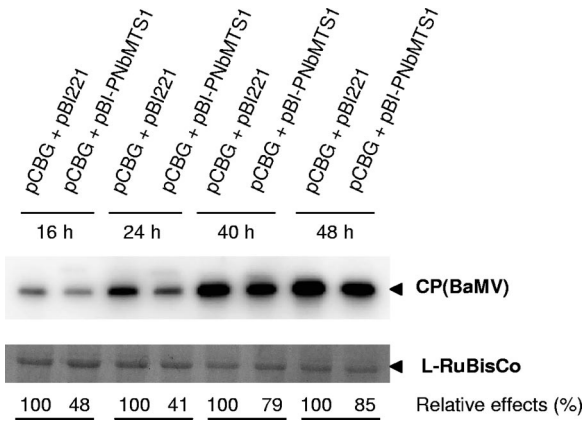

FIG. 5. Time course of the inhibitory effect of PNbMTS1 on BaMV accumulation. Protoplasts of *N. benthamiana* were transfected with 2.5 μg pCBG and 7.5 μg pBI221 or pBI-PNbMTS1 as indicated. Cells were collected at the indicated times of incubation and subjected to analyses for total protein contents and BaMV coat protein accumulation. The relative effects were estimated based on the corresponding pixels of coat proteins after normalization to the amounts of L-RuBisCo.

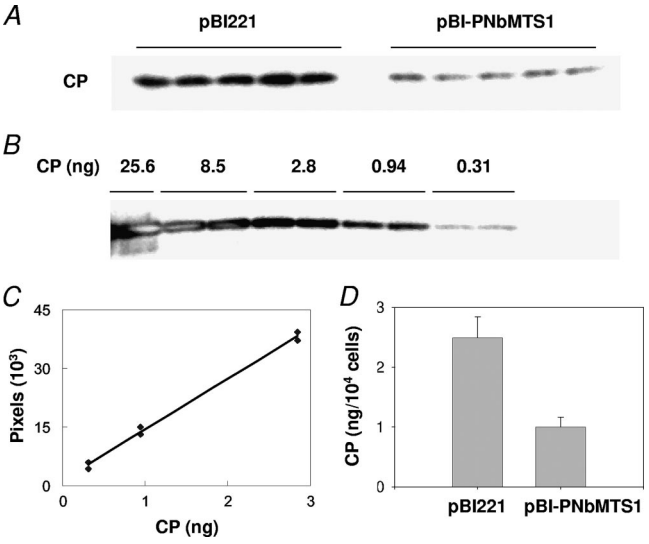

FIG. 6. Quantitative analysis of BaMV coat protein accumulated in protoplasts. Protoplasts of *N. benthamiana* were transfected with 2.5 μg pCBG and 10 μg pBI221 or pBI-PNbMTS1 and incubated for 16 h. The accumulation of BaMV coat protein was analyzed by Western blotting (A) and calculated according to a standard curve of dilutions of known amounts of BaMV coat protein versus pixels (B and C). Panels A and B were obtained from the same blot. Panel D shows the difference in the amounts of the coat protein in protoplasts cotransfected with pBI221 or pBI-PNbMTS1 after normalization to the amounts of L-RuBisCo. Error bars indicate standard deviations.

antibody. The results showed that BaMV RdRp could be coprecipitated by the anti-GFP antibody if pBI-PNbMTS1/GFP, but not pBI-GFP, had been cointroduced with pBI-RdRpHA into protoplasts (Fig. 7). PNbMTS1/GFP and GFP actually could be expressed in protoplasts, and the presence of the former

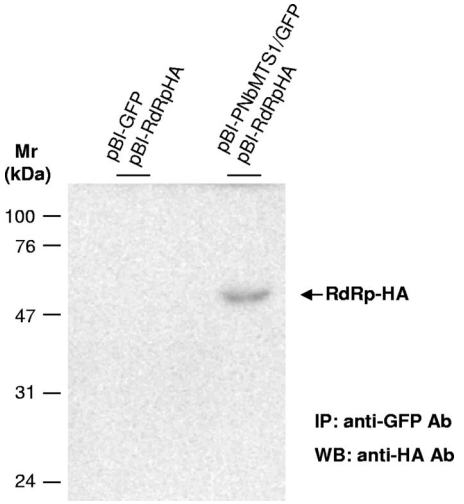

FIG. 7. Interaction of BaMV RdRp domain and PNbMTS1 in protoplasts. Protoplasts transfected with pBI-RdRpHA and pBI-GFP (or pBI-PNbMTS1/GFP) were disrupted, and their membrane fractions were collected by 1 h of centrifugation at 30,000 × *g*. The proteins in the fraction were solubilized in NP-40-containing buffer and incubated with rabbit anti-GFP antibody (Ab) and protein-A Sepharose. The immunoprecipitated (IP) proteins were then analyzed by Western blotting (WB) using mouse anti-HA antibody as the primary antibody.

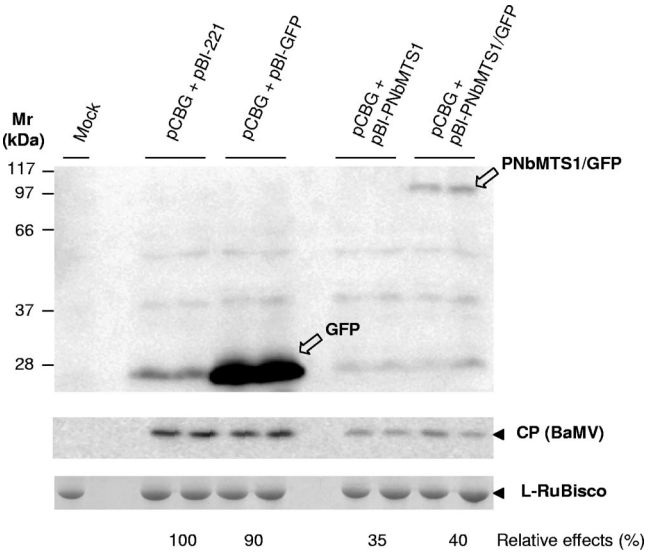

FIG. 8. Expression of PNbMTS1/GFP in protoplasts and its inhibitory effect on the accumulation of BaMV coat protein. Protoplasts of *N. benthamiana* were transfected with 5 μg of pCBG and 15 μg of the indicated plasmids derived from pBI221. After 18 h of incubation at ambient temperature, the protoplasts were harvested and specified proteins in the extracts were analyzed by SDS-PAGE and Western blotting. Anti-GFP antibody was used for the detection of PNbMTS1/GFP and GFP. Experiments were performed in duplicate. The relative effects were estimated based on the corresponding pixels of coat proteins after normalization to the amounts of L-RuBisCo.

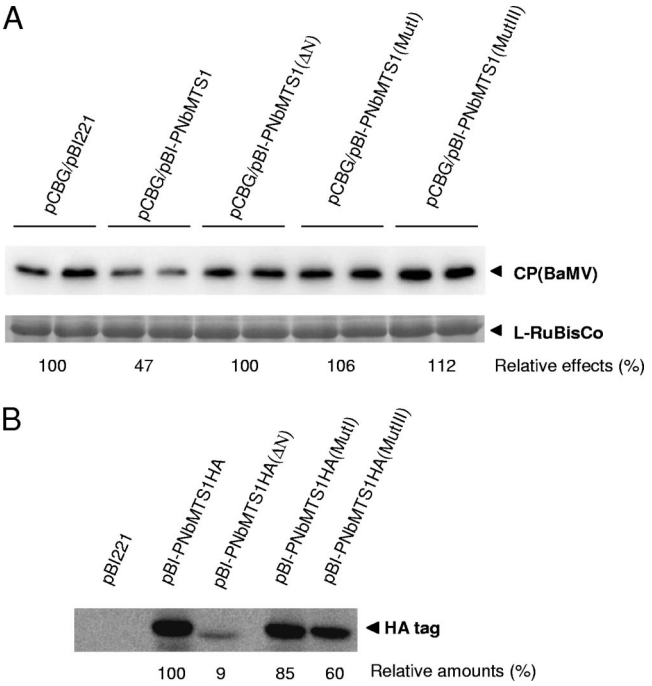

FIG. 9. Mutational effects of PNbMTS1 on BaMV accumulation. (A) Protoplasts of *N. benthamiana* were transfected with 3.5 μg pCBG and 3.5 μg pBI221 or its derivatives and incubated under the conditions described in Materials and Methods. The total protein contents and accumulation of BaMV coat protein (CP) in the transfected protoplasts were analyzed at 16 h posttransfection. Plasmid pBI-PNbMTS1(ΔN) encodes an N-terminally truncated PNbMTS1, whereas pBI-PNbMTS1(MutI) and pBI-PNbMTS1(MutIII) produce mutant proteins bearing G215A/G217A and G302A/G303A double mutations, respectively. Experiments were performed in duplicate. (B) Protoplasts of *N. benthamiana* were transfected with the indicated plasmids, and the expression of C-terminally HA-fused PNbMTS1 and its derivatives was detected by Western blotting using anti-HA antibody as the primary antibody. The relative values of pixels corresponding to the accumulations of BaMV coat protein and HA tag-fused proteins are indicated in panels A and B, respectively. The relative effects were estimated based on the corresponding pixels of coat proteins after normalization to the amounts of L-RuBisCo.

also resulted in a decrease in the accumulation of BaMV coat protein, suggesting analogous functions of PNbMTS1/GFP and PNbMTS1 (Fig. 8).

Significance of AdoMet in PNbMTS1 function. Analysis of the amino acid sequence of PNbMTS1 revealed two motifs similar to the consensus AdoMet-binding motifs I, (L/I/V)(V/L)(E/D)(V/I)G(G/C)G(P/T)G, and III, LL(K/R)PGG(L/I/R)(I/L)(V/I/F/L)(V/L/I), of diverse AdoMet-dependent methyltransferases (Fig. 2). Therefore, it would be interesting to know the importance of the putative motifs in the viral suppression function of PNbMTS1. Two glycine residues in each of the motifs were replaced with alanines to address this issue. Also, the N-terminal 36 amino acid residues were deleted in another mutant to examine the importance of the predicted transmembrane segment (or signal peptide). The negative effect of PNbMTS1 on BaMV coat protein accumulation was abolished in response to either mutation at the putative AdoMet-binding motifs and to the deletion of the N-terminal sequence (Fig. 9A). Factors such as improper protein targeting, protein instability, and loss of the activity to bind AdoMet, may contribute to the effects observed with the BaMV coat protein. To clarify this situation, accumulation of HA-tagged PNbMTS1 variants in protoplasts was examined (Fig. 9B). The accumulation of the N-terminally truncated PNbMTS1 was significantly decreased. Conversely, the proteins bearing mutations at the putative AdoMet-binding motifs accumulated to amounts approximately equal to wild type. Collectively, the putative AdoMet-binding motifs on PNbMTS1 are critical for the BaMV suppression function. Two explanations, at least, may underlie this result. Simply, an AdoMet-binding event can sequester AdoMet from the viral mRNA capping enzyme, so that the 5′ cap structure cannot properly form on the viral RNA transcripts. Alternatively, the activity of transmethylation could be the determinant for the suppression function of PNbMTS1. A previous report stated that application of 1 mM AdoMet to *A. thaliana* protoplasts downregulates the expression of cystathionine γ-synthase (7), suggesting that AdoMet can be taken up by plant protoplasts. Accordingly, AdoMet was added to the protoplast incubation medium to clarify which is the better explanation for the inhibitory effect of PNbMTS1. The inhibition of BaMV accumulation should be alleviated under this incubation condition if sequestration mechanism plays a role. Otherwise, extra AdoMet may enhance the enzymatic activity of overexpressed PNbMTS1, leading to more inhibition of BaMV accumulation. The experiment showed that the addition of AdoMet further decreased the coat protein accumulation if pBI-PNbMTS1 had been introduced into protoplasts (Fig. 10). The result also indicated that extra AdoMet did not exert a significant negative effect on the

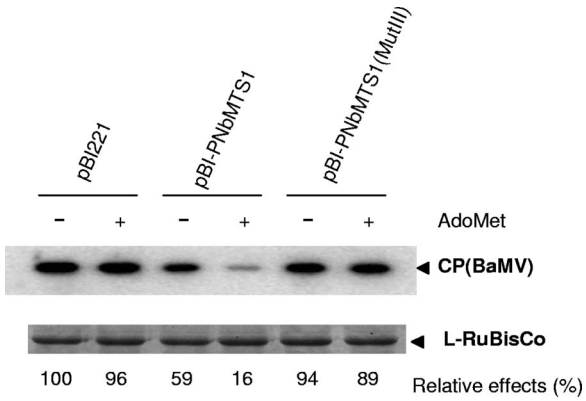

FIG. 10. AdoMet dependence of the inhibitory effect of PNbMTS1. Protoplasts of *N. benthamiana* were transfected with 2.5 μg pCBG and 7.5 μg pBI221 or its derivatives and incubated under the conditions described in Materials and Methods. The total protein contents and accumulation of BaMV coat protein (CP) in the transfected protoplasts were analyzed at 16 h posttransfection. Some incubation media were supplemented with 0.32 mM AdoMet as indicated. The relative effects were estimated based on the corresponding pixels of coat proteins after normalization to the amounts of L-RuBisCo.

accumulation of BaMV coat protein in protoplasts cotransfected with pBI-PNbMTS1(MutIII) or pBI221.

Virus specificity of the PNbMTS1 function. The course from pCBG in the nucleus to the self-replicating viral RNA transcript in the cytoplasm involves steps such as 35S promoter-based transcription and nuclear export of the pCBG-derived transcript. Adverse effects on any of the steps by PNbMTS1 may result in decreases in the viral coat protein accumulation. It was therefore important to determine whether similar effects could be observed when the RNA genome from the BaMV virion was introduced into protoplasts (Fig. 11A). The results indicated that PNbMTS1 decreased the accumulation of BaMV coat protein regardless of whether the protoplasts were initially transfected with pCBG or the viral genomic RNA. To

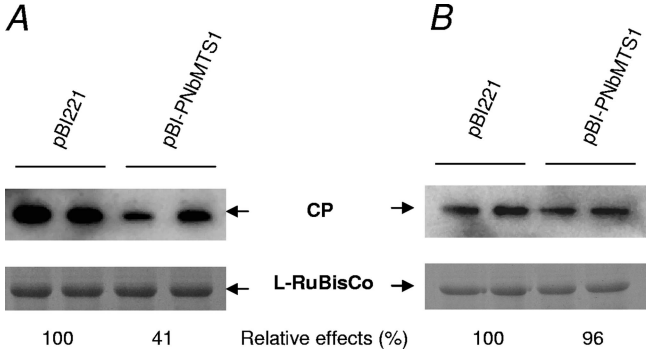

FIG. 11. Specificity of the inhibitory effect of PNbMTS1. Protoplasts of *N. benthamiana* were transfected with 0.3 μg genomic RNA of BaMV and 3 μg pBI221 or pBI-PNbMTS1 (A) or with 1 μg genomic RNA of TMV and 10 μg pBI221 or pBI-PNbMTS1 (B) and incubated under the conditions described in Materials and Methods. The protein contents and accumulation of the specific viral coat protein in protoplasts were analyzed after 16 h of incubation. Experiments were performed in duplicate. The relative effects were estimated based on the corresponding pixels of the specified coat proteins after normalization to the amounts of L-RuBisCo.

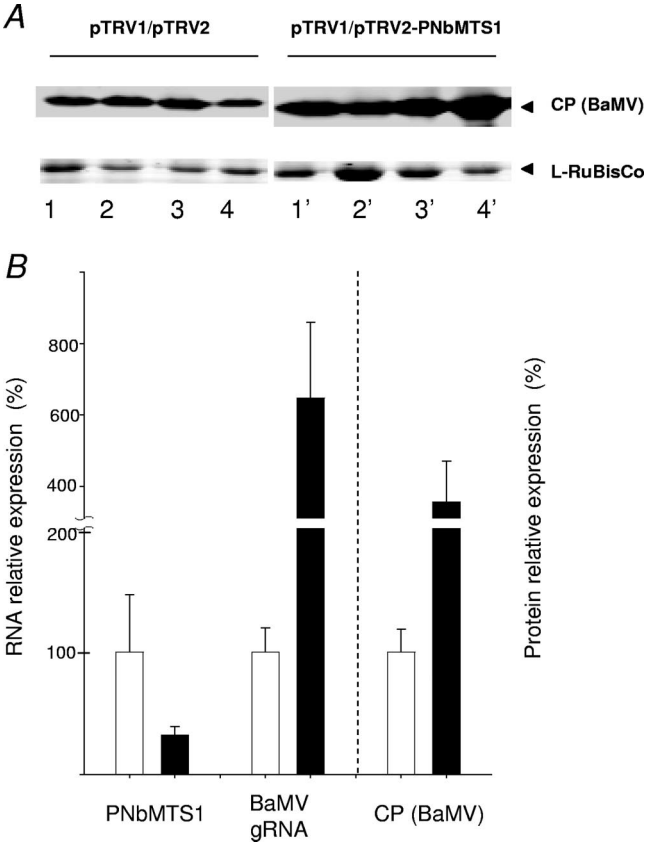

FIG. 12. Enhancement of BaMV accumulation in PNbMTS1-silenced *N. benthamiana*. Endogenous PNbMTS1 in *N. benthamiana* was suppressed by RNA interference techniques as described in Materials and Methods. (A) Accumulation of BaMV coat protein in PNbMTS1-silenced hosts and controls. Each lane number represents an individual plantlet and the two sets of data were obtained from the same blot. (B) Relative amounts of mRNA transcripts of PNbMTS1 and BaMV genomic RNA and the viral coat protein (CP) in PNbMTS1-silenced hosts (closed bars) and controls (open bars). The measurement of RNA transcripts was carried out using real-time PCR and normalized by the expression of GAPDH, whereas BaMV coat protein was analyzed by Western blotting and normalized by the amounts of L-RuBisCo. Error bars indicate standard deviations.

examine whether PNbMTS1 has a specific effect on BaMV replication, the RNA genome from TMV virions was also included in the test (Fig. 11B). The accumulation of TMV coat protein was not significantly affected by PNbMTS1.

BaMV accumulation in PNbMTS1-silenced *N. benthamiana*. Since overexpression of PNbMTS1 decreased BaMV accumulation in protoplasts, we asked whether BaMV replication would be increased by silencing PNbMTS1. Silencing of PNbMTS1 was achieved by the VIGS technique using *Tobacco rattle virus* vectors as described in Materials and Methods. After silencing treatment, the newly developed leaves were then inoculated with BaMV virions and the effect on viral accumulation was followed. As expected, accumulation of BaMV coat protein in PNbMTS1-silenced plants was higher than that in control plants by 3.7-fold (Fig. 12A). Relative quantification of RNA transcripts by real-time RT-PCR also revealed six times more BaMV genomic RNA, but only ~35% PNbMTS1 transcripts, in PNbMTS1-silenced plants compared

with control plants by using GAPDH transcripts as the internal control (Fig. 12B). Similar results were obtained when mitochondrial 18S RNA was used as the internal control. The results are in agreement with the suggestion that the PNbMTS1 is a suppressor of BaMV accumulation. It should be noted that the silencing treatment did not cause noticeable changes in the plant's appearance.

DISCUSSION

AdoMet-dependent methyltransferases comprise a large group of enzymes involved in a variety of biological functions, such as biosynthesis, signal transduction, protein repair, chromatin regulation, and gene silencing. They catalyze transfer of methyl groups to various substrates, including proteins, nucleic acids, and metabolic compounds, by using AdoMet as the methyl donor. Protein methylation is also implicated in the life cycles of viruses in diverse ways. Methylation at arginine residues of the RNA-binding motif of a small form of *Hepatitis delta virus* antigen is required for viral replication (25). Arginine methylation of adenovirus E1B-AP5 protein is also crucial for the virus to replicate efficiently (19). During preparation of this paper, a novel protein arginine methyltransferase in *Nicotiana tabacum* was reported to methylate *Cucumber mosaic virus* 1a protein and promote viral spread to noninoculated upper leaves (15). On the other hand, methylation of viral proteins may negatively affect viral replication. For instance, methylation of Tat protein of human immunodeficiency virus type 1 by PRMT6 decreases the interaction of the protein with the Tat transactivation region of viral RNA, leading to a reduction in cyclin T1-dependent Tat transcriptional activation (33). RNA methylation is also implicated in the pathogenesis of plant viruses. Methylation of micro-RNAs at the 2′-OH of the 3′-terminal nucleotide by HEN1 is crucial for the biogenesis of the small RNA molecules (21, 35), and this activity could be interrupted by viral RNA silencing suppressors p21, p19, and P1/HC-Pro (36).

PNbMTS1 was identified in a yeast two-hybrid screening owing to its ability to bind to the BaMV RdRp. The physiological function of PNbMTS1 and its homologues in other plants has hitherto not been characterized. Two lines of evidence indicate an inhibitory role for PNbMTS1 in BaMV accumulation. First, overexpression of the protein decreased the accumulation of the viral coat protein in protoplasts; second, suppression of the protein, by VIGS, increased the viral coat protein as well as the viral genomic RNA in plants. PNbMTS1 may therefore take part in the plant defense networks counteracting the viral infection. Coimmunoprecipitation suggests an association between PNbMTS1 and the viral RdRp domain in protoplasts; however, whether the interaction itself is crucial for the inhibitory effect remains to be addressed. Other questions such as the intracellular location of PNbMTS1 and its expression profile and responsiveness upon BaMV infection are also worth being investigated.

Deletion of the N-terminal 36 amino acids decreased the accumulation of PNbMTS1. Misfolding and the resulting destabilization of the protein may account for this result. Also, proper targeting of PNbMTS1 may be relevant to its viral suppression function. The chloroplast membrane has been suggested to be the site for BaMV replication based on the finding that the chloroplast phosphoglycerate kinase can assist viral replication (26). However, direct evidence for this is still lacking. The inhibitory effect of PNbMTS1 on the viral accumulation probably depends on the protein's catalytic function, because the AdoMet-binding motifs are required for the inhibition and AdoMet augments the effect. This conclusion inevitably leads to an important question as to what mechanism underlies this inhibitory effect. Is it possible that PNbMTS1 exerts its function through methylation directly on the viral RdRp or the viral genome or indirectly on some other cellular factors involved in the uncharacterized viral replication complex? To address this issue, we have incubated the protoplasts cotransfected with pBI-PNbMTS1 and pBI-RdRpHA in Ado[*methyl*-^{14}C]Met-containing medium and examined whether the HA-tagged RdRp was radiolabeled. The radioactive signal on the protein was rather weak (data not shown); therefore, we still do not have an affirmative answer for the question of whether the viral RdRp domain could be methylated by PNbMTS1. We have also tried to express PNbMTS1 in *E. coli* in order to characterize its in vitro enzymatic activity. Unfortunately, this attempt has not succeeded yet due to the insolubility of the protein in *E. coli*.

In conclusion, PNbMTS1 was found to interact with the RdRp domain of BaMV, and it had a negative effect on viral accumulation. PNbMTS1 may represent a novel component of the plant defense network acting through a mechanism waiting to be elucidated.

ACKNOWLEDGMENTS

This work was supported by grants NSC 94-2752-B-005-012-PAE, NSC 95-2752-B-005-011-PAE, and NSC 96-2752-B-005-011-PAE from the National Science Council, Taiwan, Republic of China.

We thank Muthukumar Nadar for the preparation of the manuscript.

REFERENCES

1. **Ahlquist, P., A. O. Noueiry, W. M. Lee, D. B. Kushner, and B. T. Dye.** 2003. Host factors in positive-strand RNA virus genome replication. J. Virol. **77:**8181–8186.
2. **Ahola, T., and P. Ahlquist.** 1999. Putative RNA capping activities encoded by brome mosaic virus: methylation and covalent binding of guanylate by replicase protein 1a. J. Virol. **73:**10061–10069.
3. **Ahola, T., and L. Kääriäinen.** 1995. Reaction in alphavirus mRNA capping: formation of a covalent complex of nonstructural protein nsP1 with 7-methyl-GMP. Proc. Natl. Acad. Sci. USA **92:**507–511.
4. **Blackwell, J. L., and M. A. Brinton.** 1997. Translation elongation factor-1α interacts with the 3′ stem-loop region of West Nile virus genomic RNA. J. Virol. **71:**6433–6444.
5. **Blumenthal, T., and G. G. Carmichael.** 1979. RNA replication: function and structure of Qβ-replicase. Annu. Rev. Biochem. **48:**525–548.
6. **Cheng, J.-H., M.-P. Ding, Y.-H. Hsu, and C.-H. Tsai.** 2001. The partial purified RNA-dependent RNA polymerases from bamboo mosaic potexvirus and potato virus X infected plants containing the template-dependent activities. Virus Res. **80:**41–52.
7. **Chiba, Y., R. Sakurai, M. Yoshino, K. Ominato, M. Ishikawa, H. Onouchi, and S. Naito.** 2003. S-Adenosyl-L-methionine is an effector in the posttranscriptional autoregulation of the cystathionine γ-synthase gene in Arabidopsis. Proc. Natl. Acad. Sci. USA **100:**10225–10230.
8. **Das, T., M. Mathur, A. K. Gupta, G. M. Janssen, and A. K. Banerjee.** 1998. RNA polymerase of vesicular stomatitis virus specifically associates with translation elongation factor-1 αβγ for its activity. Proc. Natl. Acad. Sci. USA **95:**1449–1454.
9. **de Nova-Ocampo, M., N. Villegas-Sepúlveda, and R. M. del Angel.** 2002. Translation elongation factor-1α, La, and PTB interact with the 3′ untranslated region of dengue 4 virus RNA. Virology. **295:**337–347.
10. **Han, Y.-T., C.-S. Tsai, Y.-C. Chen, M.-K. Lin, Y.-H. Hsu, and M. Meng.** 2007. Mutational analysis of a helicase motif-based RNA 5′-triphosphatase/NTPase from bamboo mosaic virus. Virology **367:**41–50.
11. **Huang, Y.-L., Y.-H. Hsu, Y.-T. Han, and M. Meng.** 2005. mRNA guanylation

catalyzed by the S-adenosylmethionine-dependent guanylyltransferase of bamboo mosaic virus. J. Biol. Chem. **280:**13153–13162.
12. **Joshi, R. L., J. M. Ravel, and A. L. Haenni.** 1986. Interaction of turnip yellow mosaic virus Val-RNA with eukaryotic elongation factor EF-1α. Search for a function. EMBO J. **5:**1143–1148.
13. **Kagan, R. M., and S. Clarke.** 1994. Widespread occurrence of three sequence motifs in diverse S-adenosylmethionine-dependent methyltransferases suggests a common structure for these enzymes. Arch. Biochem. Biophys. **310:**417–427.
14. **Katz, J. E., M. Dlakic, and S. Clarke.** 2003. Automated identification of putative methyltransferases from genomic open reading frames. Mol. Cell Proteomics **2:**525–540.
15. **Kim, M. J., S. U. Huh, B.-K. Ham, and K.-H. Paek.** 2008. A novel methyltransferase methylates *Cucumber mosaic virus* 1a protein and promotes systemic spread. J. Virol. **82:**4823–4833.
16. **Kiyosue, T., K. Yamaguchi-Shinozaki, and K. Shinozaki.** 1994. Cloning of cDNAs for genes that are early-responsive to dehydration stress (ERDs) in *Arabidopsis thaliana* L.: identification of three ERDs as HSP cognate genes. Plant Mol. Biol. **25:**791–798.
17. **Kong, F., K. Sivakumaran, and C. Kao.** 1999. The N-terminal half of the *Brome mosaic virus* 1a protein has RNA capping-associated activities: specificity for GTP and *S*-adenosylmethionine. Virology **259:**200–210.
18. **Kushner, D. B., B. D. Lindenbach, V. Z. Grdzelishvili, A. O. Noueiry, S. M. Paul, and P. Ahlquist.** 2003. Systematic, genome-wide identification of host genes affecting replication of a positive-strand RNA virus. Proc. Natl. Acad. Sci. USA **100:**15764–15769.
19. **Kzhyshkowska, J., E. Kremmer, M. Hofmann, H. Wolf, and T. Dobner.** 2004. Protein arginine methylation during lytic adenovirus infection. Biochem. J. **383:**259–265.
20. **Lai, M. M.** 1998. Cellular factors in the transcription and replication of viral RNA genomes: a parallel to DNA-dependent RNA transcription. Virology **244:**1–12.
21. **Li, J., Z. Yang, B. Yu, J. Liu, and X. Chen.** 2005. Methylation protects miRNAs and siRNAs from a 3′-end uridylation activity in Arabidopsis. Curr. Biol. **15:**1501–1507.
22. **Li, Y.-I., Y.-M. Cheng, Y.-L. Huang, C.-H. Tsai, Y.-H. Hsu, and M. Meng.** 1998. Identification and characterization of the *Escherichia coli*-expressed RNA-dependent RNA polymerase of bamboo mosaic virus. J. Virol. **72:** 10093–10099.
23. **Li, Y.-I., Y.-J. Chen, Y.-H. Hsu, and M. Meng.** 2001. Characterization of the AdoMet-dependent guanylyltransferase activity that is associated with the N terminus of bamboo mosaic virus replicase. J. Virol. **75:**782–788.
24. **Li, Y.-I., T.-W. Shih, Y.-H. Hsu, Y.-T. Han, Y.-L. Huang, and M. Meng.** 2001. The helicase-like domain of plant potexvirus replicase participates in formation of RNA 5′ cap structure by exhibiting RNA 5′-triphosphatase activity. J. Virol. **75:**12114–12120.
25. **Li, Y.-J., M. R. Stallcup, and M. M. Lai.** 2004. Hepatitis delta virus antigen is methylated at arginine residues, and methylation regulates subcellular localization and RNA replication. J. Virol. **78:**13325–13334.
26. **Lin, J.-W., M.-P. Ding, Y.-H. Hsu, and C.-H. Tsai.** 2007. Chloroplast phosphoglycerate kinase, a gluconeogenetic enzyme, is required for efficient accumulation of Bamboo mosaic virus. Nucleic Acid Res. **35:**424–432.
27. **Lin, N.-S., B.-Y. Lin, N.-W. Lo, C.-C. Hu, T.-Y. Chow, and Y.-H. Hsu.** 1994. Nucleotide sequence of the genomic RNA of bamboo mosaic potexvirus. J. Gen. Virol. **75:**2513–2518.
28. **Magden, J., N. Takeda, T. Li, P. Auvinen, T. Ahola, T. Miyamura, A. Merits, and L. Kääriäinen.** 2001. Virus-specific mRNA capping enzyme encoded by hepatitis E virus. J. Virol. **75:**6249–6255.
29. **Panavas, T., E. Serviene, J. Brasher, and P. D. Nagy.** 2005. Yeast genome-wide screen reveals dissimilar sets of host genes affecting replication of RNA viruses. Proc. Natl. Acad. Sci. USA **102:**7326–7331.
30. **Ratcliff, F., A. M. Martin-Hernandez, and D. C. Baulcombe.** 2001. Tobacco rattle virus as a vector for analysis of gene function by silencing. Plant J. **25:**237–245.
31. **Sheen, J.** 2001. Signal transduction in maize and Arabidopsis mesophyll protoplasts. Plant Physiol. **127:**1466–1475.
32. **Wang, X., Z. Ullah, and R. Grumet.** 2000. Interaction between zucchini yellow mosaic potyvirus RNA-dependent RNA polymerase and host poly-(A) binding protein. Virology **275:**433–443.
33. **Xie, B., C. F. Invernizzi, S. Richard, and M. A. Wainberg.** 2007. Arginine methylation of the human immunodeficiency virus type 1 Tat protein by PRMT6 negatively affects Tat interactions with both cyclin T1 and the Tat transactivation region. J. Virol. **81:**4226–4234.
34. **Yamaji, Y., T. Kobayashi, K. Hamada, K. Sakurai, A. Yoshii, M. Suzuki, S. Namba, and T. Hibi.** 2006. In vivo interaction between tobacco mosaic virus RNA-dependent RNA polymerase and host translation elongation factor 1A. Virology **347:**100–108.
35. **Yu, B., Z. Yang, J. Li, S. Minakhina, M. Yang, R. W. Padgett, R. Steward, and X. Chen.** 2005. Methylation as a crucial step in plant microRNA biogenesis. Science **307:**932–935.
36. **Yu, B., E. J. Chapman, Z. Yang, J. C. Carrington, and X. Chen.** 2006. Transgenically expressed viral RNA silencing suppressors interfere with microRNA methylation in Arabidopsis. FEBS Lett. **580:**3117–3120.
37. **Zeenko, V. V., L. A. Ryabova, A. S. Spirin, H. M. Rothnie, D. Hess, K. S. Browning, and T. Hohn.** 2002. Eukaryotic elongation factor 1A interacts with the upstream pesudoknot domain in the 3′ untranslated region of tobacco mosaic virus RNA. J. Virol. **76:**5678–5691.